

# A Single DNA Molecule Nanomotor

Jianwei J. Li and Weihong Tan\*

Center for Research at the Bio-nano Interface, Department of Chemistry and the McKnight Brain Institute, University of Florida, Gainesville, Florida 32611

Received December 26, 2001

## ABSTRACT

Nanomotors consisting of single protein molecules are abundant in living systems. Here we report a nanomotor made of a single DNA molecule. The DNA nanomotor can adopt two distinct conformations, intramolecular tetraplex and intermolecular duplex. The nanomotor switches between the two conformations through alternating DNA hybridization and strand exchange reactions, which enables the nanomotor to perform an inchworm like extending–shrinking motion. When the single molecule nanomotor is loaded with two organic molecules, a fluorophore and a quencher, the motion can be viewed in real time by monitoring the fluorescent signal. The DNA nanomotor functions efficiently both in solution and on nanoparticle surfaces. Its simple yet stable structure, convenient operation, and high efficiency may make the DNA nanomotor practically useful for powering nanosystems in future applications.

With the advancement of nanotechnology, nanomotors are required to power nanometer-scale devices.<sup>1</sup> Thus, there is a great need for various nanomotors. In living organisms exist plentiful natural nanomotors to help maintain cellular structure and function by performing diverse subtle motions.<sup>2</sup> On the other hand, great effort has been made recently toward the design and synthesis of artificial nanomotors.<sup>3</sup> While most of the synthetic nanomotors are based on small organic molecules, recent advancements have led to the emergence of DNA nanomotors as a new nanomotor family.<sup>4</sup> These DNA nanomotors are constructed through self-assembly of several DNA strands and produce twisting or opening-closing movements. In this report a nanomotor consisting of a single DNA molecule is constructed and tested.

The working principle of the single molecule nanomotor is shown in Figure 1. The nanomotor is a 17mer DNA oligonucleotide. On its own, the 17mer folds into a unimolecular tetraplex (or quadruplex) structure,<sup>5</sup> in which its two ends are kept close to each other. This is the nanomotor's shrunken state. In the presence of a complementary sequence,  $\alpha$  (5'-GTA GTC CGC GAC CAA CCA CAC CAA CCA-3'), the 17mer and  $\alpha$  form a double stranded DNA, straightening the tetraplex and separating the two ends away from each other (I). This is the nanomotor's extended state. The nanomotor returns to its shrunken state through a strand exchange reaction<sup>6</sup> in which the 17mer is displaced by a longer strand,  $\beta$  (5'-TGG TTG GTG TGG TTG GTC GCG GAC TAC-3'). The strand exchange reaction is initiated by DNA sticky end pairing (II)<sup>7</sup> and proceeds through branch migration.<sup>8</sup> The newly formed duplex DNA,  $\alpha\beta$ , is longer and more stable, driving the strand exchange reaction to completion (III). The released 17mer forms the shrunken tetraplex of the nanomotor (IV), finishing one extending–

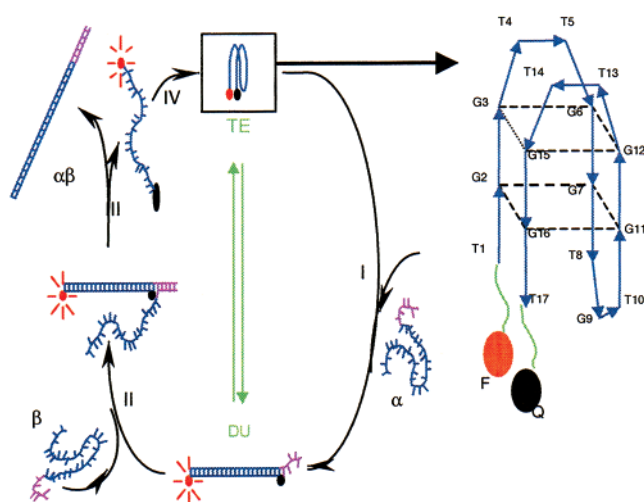


**Figure 1.** 17mer DNA nanomotor (T1G2G3T4T5G6G7T8G9T10G11G12T13T14G15G16T17) can adopt an intramolecular tetraplex (TE) conformation, as indicated by the thick arrow. It extends into duplex (DU) when it hybridizes to strand  $\alpha$  and shrinks back to TE when strand  $\alpha$  is displaced via hybridization with strand  $\beta$ . The blue portion in  $\alpha$  is complementary to the nanomotor, and the purple portion represents extra bases to form sticky ends in DU.  $\alpha$  and  $\beta$  are totally complementary to each other. A fluorophore (red ball) and a quencher (black ball) are connected through two linkers (green lines) to the ends of the 17-mer to report the motion of the nanomotor, which is shown as two layers of G tetrads.<sup>5</sup>

shrinking cycle. Adding more  $\alpha$  will start a new cycle. Since this nanomotor switches between duplex (abbreviated to “DU”) and tetraplex (abbreviated to “TE”), we call it a “DUTE nanomotor”.

Each cycle of a DUTE nanomotor produces a waste molecule,  $\alpha\beta$ , and thus the consumed energy equals the decrease in free energy during the hybridization between  $\alpha$

and  $\beta$ . This energy is the total driving force for the nanomotor's cycling and can be converted into mechanical movement of loads when the nanomotor is loaded. As an example to demonstrate the principle and for easy monitoring of the motor's movement, here we load two molecules, one fluorophore and one quencher, to the two ends of the nanomotor (Figure 1). These special loads provide us a sensitive signal transduction mechanism for real-time observation of the nanomotor's mechanical movements.<sup>9</sup> In the shrunken state, the fluorophore and quencher are drawn close to each other and thus the fluorescence is quenched through fluorescence energy transfer;<sup>9</sup> in the extended state the two moieties are separated and the fluorophore lights up (Figure 1).

To confirm that the DUTE nanomotor does work in the way shown in Figure 1, we first show that it can form both TE and DU structures. A 15mer G-rich sequence, GGTTG-GTGTGGTTGG, has been reported to adopt a highly compact tetraplex structure containing two guanine tetrads and three loops.<sup>8</sup> The DUTE nanomotor is the result of adding one thymine to each end of the 15mer. Here the two thymine bases are added to buffer potential interference of the loads upon the formation of TE structure. Below we show, through two experiments, that the loaded nanomotor can form TE, and, moreover, the TE can be straightened into DU.

In the first experiment, we have probed the DUTE nanomotor's conformational conversion by observing its fluorescence signal change. It is known  $K^+$  ion can promote the conversion of a G-rich sequence from loose random coil into compact TE.<sup>5</sup> For the loaded nanomotor, such a conversion will lead to fluorescence quenching. When  $K^+$  was added, we observed the fluorescence of the nanomotor solution dropped by over 80%, while a similarly labeled scrambled 17mer (S17mer), not expected to form TE, did not show any significant quenching. This indicates that the DUTE nanomotor forms TE. It is noteworthy that even in the absence of  $K^+$ , the fluorescence intensity of the DUTE nanomotor is already only 70% of that of the S17mer. This suggests the loaded DUTE nanomotor partially forms TE at room temperature without the help of  $K^+$ , implicating the strong tendency of the nanomotor to form TE. Next we show the shrunken TE can be straightened into DU upon hybridization to its complementary sequence. When we added strand  $\alpha$  into the solution of the DUTE nanomotor, the nanomotor's fluorescence intensity was enhanced by over 9 times (Figure 2), indicating the formation of a double stranded DNA. As expected, the DUTE nanomotor and S17mer have similar fluorescence intensity when they are in the DU form. In their DU form, the nanomotor and the S17mer showed higher fluorescence intensity than that in their initial state in which no ion was added. This is because the fluorophore-quencher separation is the largest in the DU form.

In the second experiment, we have further confirmed the capability of the loaded DUTE nanomotor to form TE and DU structures. The nanomotor's TE and DU forms were analyzed by nondenaturing gel electrophoresis in the presence

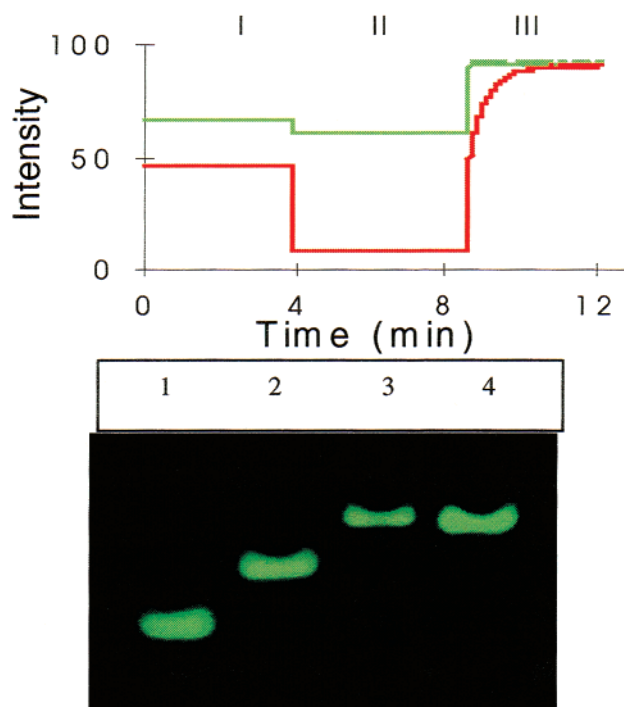


**Figure 2.** (a) Fluorescent response of the nanomotor 17mer (red) and the S17mer (green) (I) to the addition of  $K^+$  (II) and to the addition of complementary sequences (III): I, no salt; II, added 10 mM  $K^+$ ; III, added  $\alpha$ . (b) Gel electrophoresis: 1, nanomotor; 2, S17mer; 3, nanomotor plus  $\alpha$ ; 4, S17mer plus its complementary sequence.

of  $K^+$ , and the fluorophore-quencher labeled S17mer and its DU form were run simultaneously as controls. As shown in Figure 2, the DUTE nanomotor apparently moved faster than the S17mer. These two oligonucleotides have the same base composition. Therefore, their difference in mobility reflects their variance in conformation. It is known that intramolecular tetraplex DNA has higher electrophoretic mobility than the corresponding random coil.<sup>10</sup> Thus the higher mobility of the DUTE nanomotor supports the above observation that the nanomotor forms a compact TE structure while the S17mer is still in a random coil state in the presence of  $K^+$ . It is noteworthy that the amount of DUTE 17mer used here is 7 times that of S17mer in order to get similar band intensities. The much weaker fluorescence intensity of the nanomotor further supports the formation of TE. In the presence of complementary sequences, the mobility of the DUTE nanomotor and that of the S17mer both decreased significantly, indicating the formation of the DU structures. The DU form of the DUTE nanomotor and that of the S17mer showed similar mobilities, reflecting their structural similarity.

Next we show that the DUTE nanomotor can be cycled continuously by switching between its two conformations. Figure 3 is the real time monitoring of the cycling of the DUTE nanomotor in the presence of 10 mM KCl. The cycling started from TE state. Similar to the result in Figure 2, the addition of  $\alpha$  led to a sharp increase in fluorescence, indicating the conversion from TE to DU. To complete one cycle, strand  $\beta$  was added. The fluorescence decrease indicated the nanomotor's release and folding back into TE.

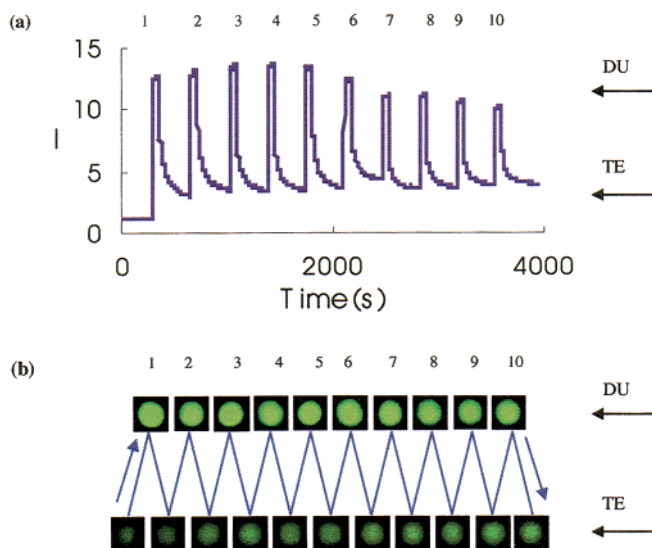


**Figure 3.** Cycling of the DNA nanomotor. During the nanomotor's cycling, the fluorescence intensity is recorded either by a spectrofluorometer (top) or by a digital camera (bottom). Ten cycles were recorded here.

Adding more strand  $\alpha$  initiated the second cycle, and so on. Ten cycles were recorded in Figure 3. The cycling of the DUTE nanomotor can also be presented by direct imaging. Figure 3 shows the fluorescence image of the nanomotor's solution during its cycling. The switching between TE and DU is simply reflected by the light and dark images. The results in Figure 3a,b are consistent with each other. The fluorescence intensity in the DU state decreased with cycling, and this was caused by the dilution effect when the solution volume increased with the addition of strand  $\alpha$  and strand  $\beta$ . On the other hand, the fluorescence intensity of the TE state increased. This might be caused by an incomplete release of the nanomotor strand. The small irregular fluctuations of the fluorescence intensities were caused by experimental error in the pipetting of  $\alpha$  and  $\beta$  solution. However, as shown below, all of these disadvantages can be overcome when the DUTE nanomotor is cycled on a solid surface.

In future application, the DUTE nanomotor needs to be connected to nanodevices, such as nanoparticles and nanowires. It is thus necessary to make sure the DUTE nanomotor still works when they are linked to these nanoelements. Here we demonstrate that the DUTE nanomotor performs extending–shrinking motion when it is immobilized on nanoparticle surface. To do this, we designed a triple-labeled DUTE nanomotor, as shown in Figure 4. The nanomotor contains a pair of fluorophore–quencher to report the nanomotor's motion. It also contains a biotin group, permitting the nanomotor to be linked to a nanoparticle coated with streptavidin.<sup>9,11</sup> These nanomotor-bearing nanoparticles were then immobilized onto the inner surface of a microchannel of which the solution of strand  $\alpha$  and  $\beta$  could flow in and out. Cycling was performed with alternating  $\alpha$  and  $\beta$  solutions flushing through the microchannel. Fluorescence images were taken each time when the solution was switched. Figure 4 shows the nanoparticles' fluorescent images during the nanomotor's 12 cyclings. The nanoparticles light up when

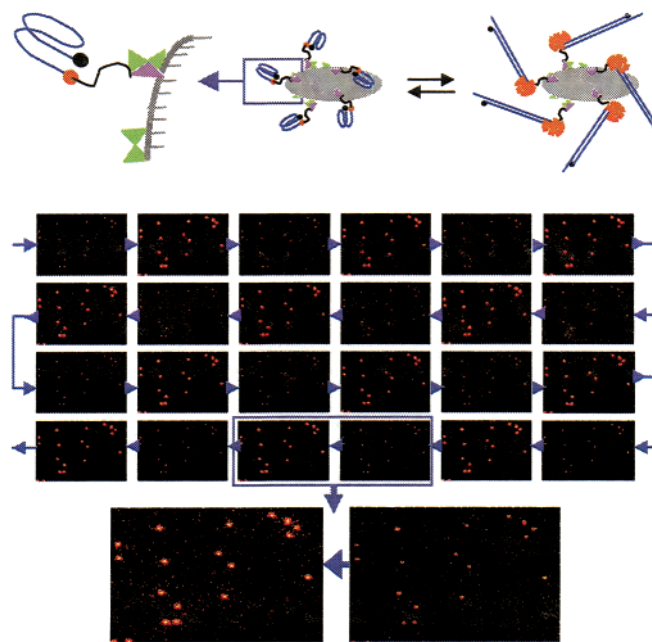


**Figure 4.** (a) Schematic representation of the triple labeled nanomotor immobilized onto nanoparticles, turning its fluorescence signal on and off upon exposure to strand  $\alpha$ /strand  $\beta$ : F, fluorophore; Q, quencher; L, linker; B, biotin; S, streptavidin; N, nanoparticle surface. (b) Images of nanoparticles with nanomotors cycling on the surface. Nanomotor-nanoparticles are immobilized onto the inner surface of a microchannel. Cycling was conducted by flushing  $\alpha$  and  $\beta$  solutions alternatively through the microchannel. The arrows indicate the order of recording the images.

solution  $\alpha$  flows through and turn dark when exposed to solution  $\beta$ . This indicates the DUTE nanomotors can still extend and shrink on the nanoparticle surface. There is no dilution effect or incomplete nanomotor release, as revealed by the consistent fluorescence intensities from image to image. The elimination of incomplete release may be due to the fact the concentration of one strand ( $\alpha$  or  $\beta$ ) is overwhelmingly higher than the other when that strand is added. This also explains why no apparent fluctuation in fluorescence intensity is observed. Given the excellent cycling capability on the surface of nanoparticles, it is reasonable to assume that the DUTE nanomotor will be useful in pulling together and pushing apart two nanoelements in a nanosystem in the future.

We have estimated the ideal energy conversion efficiency,  $f$ , which is dependent on the length of the sticky end in strand  $\alpha$ . For a 10 base long sticky end,  $f$  is 0.63, while  $f$  rises to 0.94 when the sticky end is shortened to 1 base. The theoretical extending force,  $F_{\text{ex}}$ , and shrinking force,  $F_{\text{sh}}$ , were also estimated. At 37 °C and with 25 mM KCl,  $F_{\text{ex}}$  and  $F_{\text{sh}}$  were calculated to be 20.7 and 2.2 pN, respectively. While the shrinking force is close to the forces determined for kinesin and myosin protein motors, the extending force is about 10 times larger than those protein nanomotors.<sup>12</sup> The forces are tunable through changing the solution conditions.

Even though our single DNA molecular motor is easily synthesized with the smallest molecular weight, it can function as an efficient molecular motor and has the potential to be used to power future nanoscale devices. The DUTE

motor may find applications in nanosystems, such as nanoscale switchers and nanochannels. They may also be used to maneuver nanoparticles<sup>11</sup> and to move microtubules. Transportation of molecules or nanodevices will become possible using the DUTE nanomotor. The simple molecular structure, well-controlled motion, long running life, and high-energy conversion efficiency make our single molecular DNA nanomotor attractive for these potential applications.

**Acknowledgment.** We thank Dr. Steve Benner at University of Florida for helpful discussion. This work is supported by NIH R01 NS39891, by a Research Corporation Cottrell Scholar award, and by NSF Career Award 9733650.

**Supporting Information Available:** Experimental details and theoretical calculation. This material is available free of charge via the Internet at <http://pubs.acs.org>.

## References

- (1) Soong, R. K.; Bachand, G. D.; Neves, H. P.; Olkhovets, A. G.; Craighead, H. G.; Montemagno, C. D. *Science* **2000**, *290*, 1555.
- (2) Schief, W. R.; Howard, J. *Curr. Opin. Cell Biol.* **2001**, *19*, Vale, R. D.; Milligan, R. A. *Science* **2000**, *288*, 88.
- (3) (a) Koumura, N.; Zijlstra, R. W.; van Delden, R. A.; Harada, N.; Feringa, B. L. *Nature* **1999**, *401*, 152. (b) Kelly, T. R.; De Silva, H.; Silva, R. A. *Nature* **1999**, *401*, 150.
- (4) (a) Mao, C.; Sun, W.; Shen, Z.; Seeman, N. C. *Nature* **1999**, *397*, 144. (b) Yurke, B.; Turberfield, A. J.; Mills, A. P.; Simmel, F. C.; Neumann, J. L. *Nature* **2000**, *406*, 605. (c) Simmel and Yurke *Phys. Rev. E* **2001**, *63*, 041913. (d) Yan, H.; et al. *Nature* **2002**, *415*, 62.
- (5) (a) Williamson, J. R. *Annu. Rev. Biophys. Biomol. Struct.* **1994**, *2*, 703. (b) Padmanabhan, K.; Padmanabhan, K. P.; Ferrara, J. D.; Sadler, J. E.; Tulinsky, A. *J. Biol. Chem.* **1993**, *268*, 17651.
- (6) Kmiec, E. B.; Holloman, W. K. *J. Biol. Chem.* **1994**, *269*, 10163.
- (7) Revet, B.; Fourcade, A. *Nucl. Acids Res.* **1998**, *26*, 2092.
- (8) Thompson, B. J.; Camien, M. N.; Warner, R. C. *Proc. Natl. Acad. Sci. U.S.A.* **1976**, *73*, 2299.
- (9) Fang, X.; Liu, X.; Schuster, S.; Tan, W. *J. Am. Chem. Soc.* **1999**, *121*, 2921–2922. Li, J. J.; Fang, X.; Schuster, S. M.; Tan, W. *Angew. Chem., Int. Ed. Engl.* **2000**, *39*, 1049. Fang, X.; Li, J.; Perlette, J.; Tan, W.; Wang, K. *Anal. Chem.* **2000**, *72*, 747A–753A.
- (10) Williamson, J. R.; Raghuraman, M. K.; Cech, T. R. *Cell* **1989**, *59*, 871.
- (11) Santra, S.; Zhang, P.; Wang, K.; Tapecc, R.; Tan, W. *Anal. Chem.* **2001**, *73*, 4988–4993. Santra, S.; et al. *Langmuir* **2001**, *17*, 2900–2906.
- (12) (a) Kuo, S. C.; Sheetz, M. P. *Science* **1993**, *260*, 232. (b) Visscher, K.; Schnitzer, M. J.; Block, S. M. *Nature* **1999**, *400*, 184.

NL015713+